

R.E.T. Report

Mark Godwin

01 August 2003

Contents

1 Overview	3
2 Previous Measurements	3
3 Initial Measurements	3
3.1 QVT Measurements	3
3.2 DTAKE Measurements	5
3.2.1 Voltage Settings	5
3.2.2 TDC settings	5
4 Cosmic Ray Data	5
5 Data Processing and Manipulation	8
6 LA.LB Measurements	9
7 Models: Corsika and Others	11
8 Conclusions and Future Plans	14
A 2003 Run Log	23
B Lenka Raska's Run Log	24
C Data Processing Procedure	26
D Plotting with PAW	27
E Move and Print Files	28

List of Figures

1	One PE Peak	6
2	Location Effect on Light Collection	7
3	Sum of Stack ADC	8
4	Variable Countrate	9
5	Separation Data	12
6	Overlap Data	13
7	Radial Dependence	15
8	Radial and Energy Dependence from a Simple Model	16
9	Energy Dependence on Muon Multiplicity at $r=0$	17
10	Energy Dependence on Muon Multiplicity at various radii	18
11	Number of Muons vs.Radius	19
12	Various Multiplicities from Corsika	20
13	Energy Distribution of Particles Produced by a Cosmic Ray	21
14	Radial Distribution of Particles Produced by a Cosmic Ray	22

List of Tables

1	Voltage Settings	5
2	Count Rates	10
3	Separation Data for LA.LB	10
4	Overlap Data for LA.LB	11

1 Overview

This report summarizes a Reaserch Experience for Teachers (RET) program conducted at the University of Missouri, Saint Louis (UMSL) under the supervision of Julia Thompson and David Kraus. The original work discussed in this report was performed between July 7, 2003 and August 1, 2003, and some comparisons are made to data collected in 2002.

The main focus of the study centered on measuring cosmic ray interactions using a previously constructed “stack” of six large detectors and two smaller scintillators. The size of each large scintillator is 0.42 m^2 . They are referred to as L1, L2, etc. The two smaller detectors, referred to as LA and LB, are smaller in size. LA is 35 cm by 17 cm, whereas LB is 47 cm by 17 cm. Details concerning the construction and operation of these scintillators may be found in other reports [1, 2, 3]. The operation of the six large detectors in conjunction with the two smaller detectors is usually referred to as “lstack” or sometimes “the stack”.

The long-term goal is to be able to use these and similar scintillators in high school settings to study very energetic cosmic rays and the showers they produce. Reasons for interest in this area are numerous. To mention a few, this allows physicists to study particles at energies greater than can be produced currently in accelerators, as well as study the origin (both location and the physical process) of these cosmic rays. A number of projects are currently underway, and a summary of these may be found in the report of Grosland [4].

2 Previous Measurements

One main effort of the work presented here was to summarize data previously taken by Lenka Raska [3] using the stack, LA, and LB. Dave Kraus constructed LA and LB, and Miss Raska used them in conjunction with the stack in a different location. The previous measurements were taken in the basement of the science building at Southern Illinois University - Edwardsville, whereas the present measurements were taken on the fourth (top) floor of the Research building at UMSL. Although one would expect little difference in muons coming from a cosmic-ray shower, because of their energy, there might be a substantial difference in the electromagnetic component. Although all information was not present, an effort was made to summarize the available data, and is presented in appendix B. Data gathered from these runs will be discussed in the subsequent sections.

3 Initial Measurements

3.1 QVT Measurements

The initial measurements performed used the QVT, that is, charge-voltage-time measurements. These are discussed in detail in Langford’s report [1], but a short summary is presented here. The QVT measurements are performed in order to find the location the the pedestal, photoelectric, and cosmic-ray peaks. The pedestal is the lowest charge that may be collected from a scintillator, a value that is not zero. The photoelectric peak, or PE for short, represents the charge collected when one photoelectron is initiated at the photocathode of the photomultiplier tube (PMT). The cosmic-ray peak is the charge collected when a true cosmic ray deposits its energy in a scintillator. To perform these measurements the following procedure was used:

1. The anode signal of the scintillator of interest is taken from the ADC and connected it to the input of the QVT module.

2. The coincidence logic module is set to the desired condition. For example LA.L1.L6
3. The output of the coincidence module is connected to the QVT gate. In this work a second coincidence module was used to “multiply” the coincidence gate. Thus, one output could be used to trigger the QVT and another could be used to start the TDC.
4. The pedestal was measured by taking all coincidence requirements out, except for one (any one) that was not being tested at the moment, and settin the QVT to external trigger. Data is collected with the QVT program for a few seconds.
5. Using an internal trigger on the QVT module, and taking all coincidence requirements out of the circuit, allows the PE peak to be determined. Again, data needs to be taken only for a few seconds.
6. The cosmic-ray peak is harder to determine. To determine its position (bin) all coincidence requirements must be in. Therefore data rates decreased significantly. When the desired condition was selected (in this study LA.L1.L6 and LB.L1.L6 were used most frequently) data was taken for many minutes. After a while a peak will emerge. Sometimes it can be identified by inspection, and sometimes the “fit guassian” utility of the QVT program was employed.
7. With the information gathered the PE/CR ratio may be established. The calculation is performed by the following formula:

$$\frac{PE}{CR} = \frac{CR - Ped}{PE - Ped}, \quad (1)$$

where CR , PE , and Ped represent the cosmic ray, photoelectric, and pedestal measurements, respectively.

8. Additionally, the PMT gain may be determined. Knowing that each bin represents 0.25 pC, and the one electron has a charge of 1.6×10^{-19} C, this factor is easily determined. For example, suppose the difference of the PE and Ped was 4 bins, and that a 5X attenuator was in use. The PMT gain would be

$$\begin{aligned} gain &= \left(4 \frac{\text{bins}}{\text{PE}}\right) (5) \left(\frac{0.25 \times 10^{-12} \text{C}}{\text{bin}}\right) \left(\frac{1e^-}{1.6 \times 10^{-19} \text{C}}\right) \\ gain &= 3.125 \times 10^7 \text{ electrons/PE} \end{aligned} \quad (2)$$

With knowledge of these numbers adjustments may be made for voltage, and the expected location of cosmic rays in the ADC histograms may be determined. It should be noted that sometimes the pedestal would not appear sharp, and might even display a “double peak.” In one of these situations, it was discovered that an attenuator connected directly to the PMT base was causing this problem, because it was not well grounded. Simply moving the attenuator to a different location along the ADC wire eliminated this problem. The QVT measurements are presented in Langford’s paper [1].

Scintillator Voltage Settings	
Detector	Voltage (V)
LA	2000
LB	1800
L1	1900
L2	2000
L3	1900
L4	2000
L5	1900
L6	2000

Table 1: Voltage settings for lstack

3.2 DTAKE Measurements

All runs saved during this summer project are cataloged in appendix A. The information there includes the run number, events, trigger, count rates, and other comments. Limitations in the data acquisition requires a five-digit run (although no such restriction is present on the Kaon computer used for data processing and analysis.) It was decided that typical run numbers would take the form YMDDR, where Y is for year, M is for month, DD is for day, and R is for run. For example, run 37241 was the first run taken on July 24, 2003. There are a few deviations to this which are noted in the run log.

3.2.1 Voltage Settings

After considerable discussion of the QVT results, the optimum voltage settings were determined, given the limitations of the power supply and splitters available. The table below summarizes these settings.

3.2.2 TDC settings

DTAKE is a program which reads CAMAC information, namely, the analog-to-digital (ADC) signals and the time-to-digital (TDC) signals. The ADC signals are taken directly from the anode of the PMTs. The TDC signals come from the dynode, are inverted, sent through a discriminator, and then sent to the TDC. Signals from the discriminator are used to establish the coincidence requirements. One of the first pieces of information to determine was how to convert the TDC channel to real time. This was accomplished by running DTAKE twice, once triggered on L5 (run 371106) and once under the same requirement except a known cable length was added before the TDC (run 371108). Using a 20 ns cable (actual length is 3.75 m, see [1] for a discussion), the TDC peak arrived in channel 1075, as compared to 675. Therefore, 20 ns equals 1075-675 channels, or 44.4 ps/bin. After consulting with David Kraus [5] it was determined that the TDC was set to 50 ps/bin.

4 Cosmic Ray Data

The stack of 6 large scintillators had been previously configured such that L1, L3, and L5 had their PMTs on one side (right), and L2, L4, and L6 to the other side (left). LA was placed on top of the stack, such that it was close and perpendicular to the right side. LB was correspondingly placed on the left side. Some pictures of this setup are available for public view at

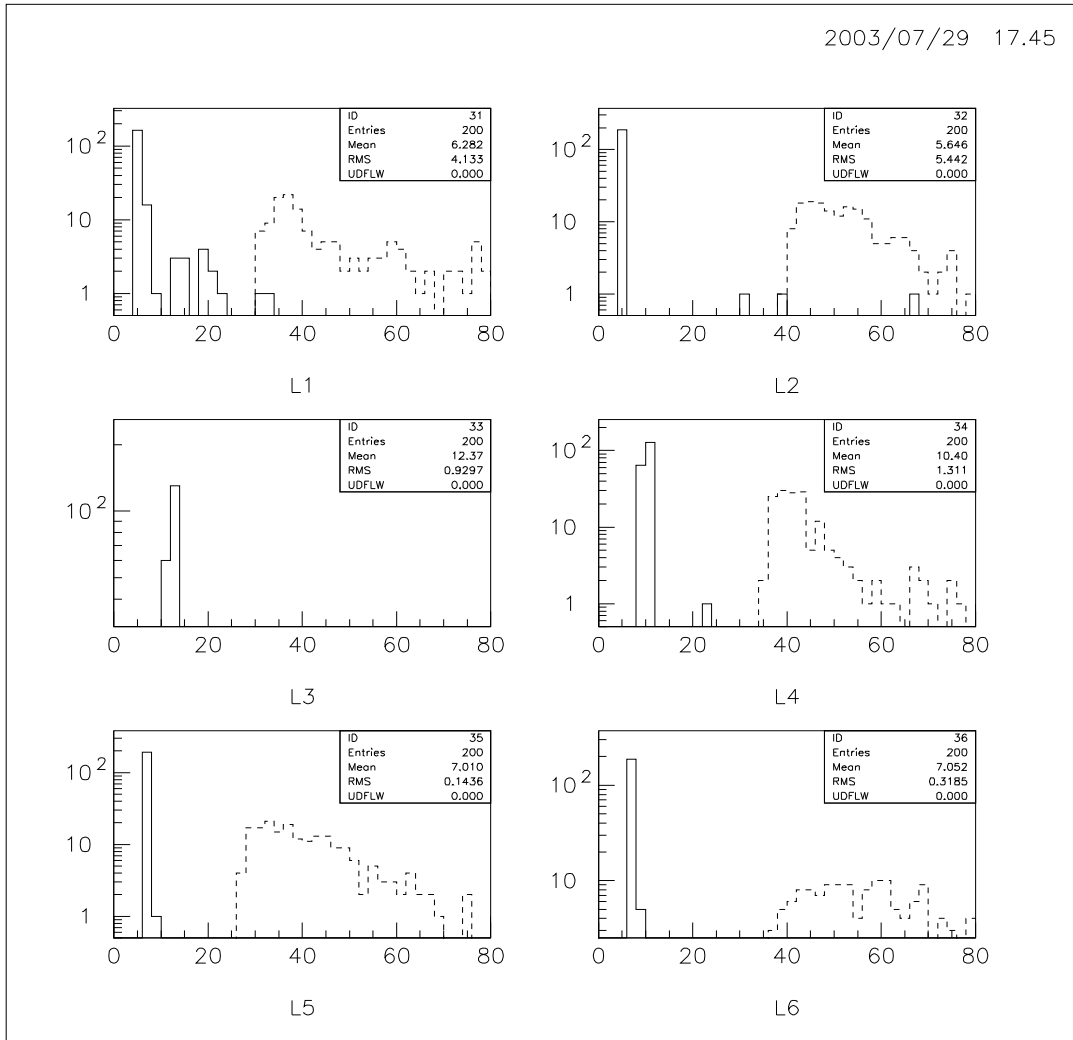


Figure 1: The plot shows the pedestal and one PE peak for each scintillator.

<http://www.phyast.pitt.edu/~jth/reupsill/2001docs/pictures/>

A series of short runs (371102-371112) were performed to examine each scintillator separately, for diagnostic purposes. No measurement of L3 was taken, because of electronics limitations. By examining this data the photoelectric peaks could be seen, and more importantly, the corresponding ADC channel. This information is shown in Fig. 1.

Additionally, longer runs were taken triggering on LA.L1.L6, and LB.L1.L6. Further details of these and all runs may be found in the run log, in appendix A. This trigger is used to ensure, as best as possible, that the data recorded comes from a cosmic ray. These runs were analyzed and display interesting, but not surprising, results. Examine Fig. 2. Displayed are the ADCs from each stack scintillator under the two coincidence requirements mentioned. This indicates that one can expect much better light collection from an ionizing particle if it is closer to the PMT.

Requiring a signal in L1 and L6 will likely result in a particle traveling through the entire stack. Thus it is meaningful to gather the energy readings from all six scintillators and add them together.

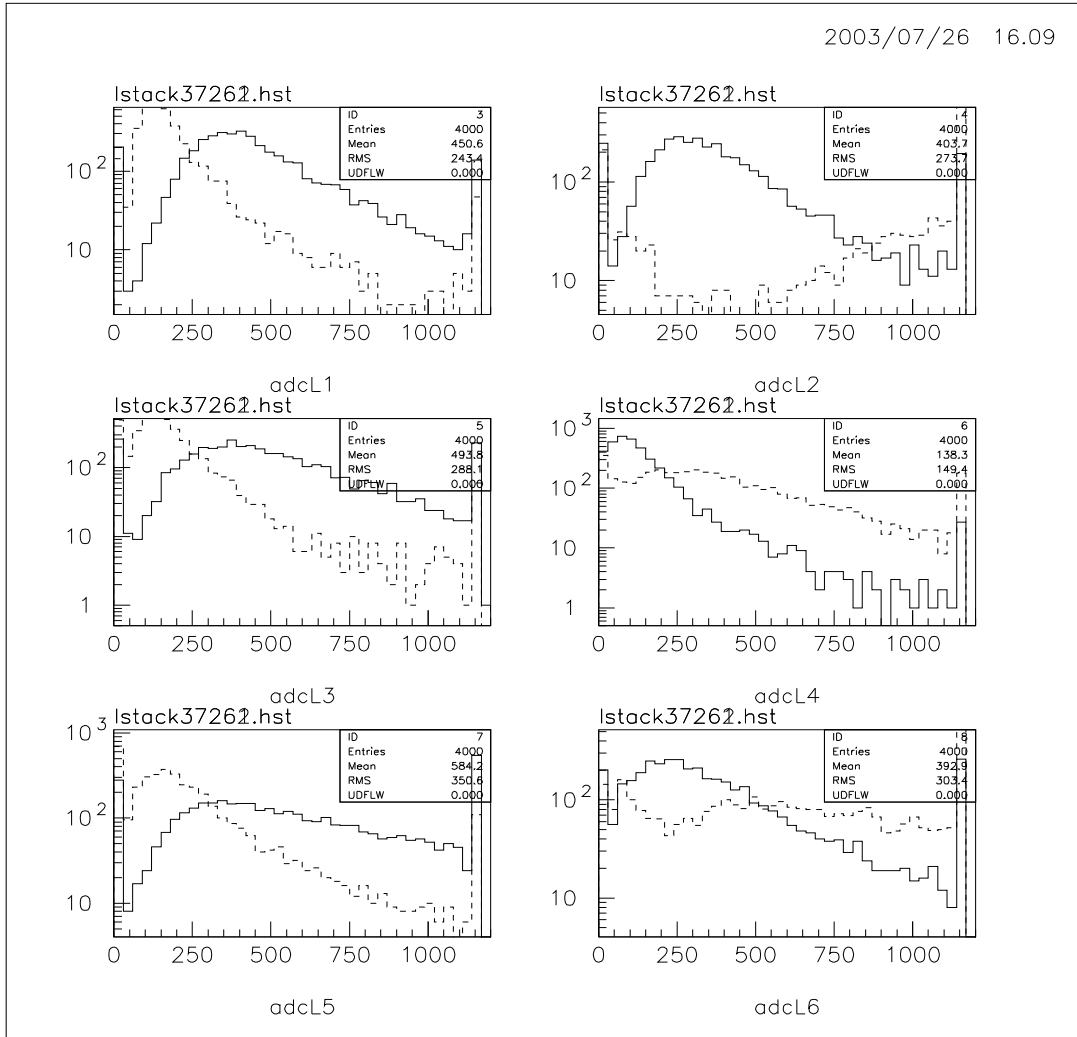


Figure 2: This figure shows how the variable light collection for the large scintillators based on the location of the interaction. Two runs are used, 37261 and 37262, the first is triggering on LA.L1.L6 and the second on LB.L1.L6.

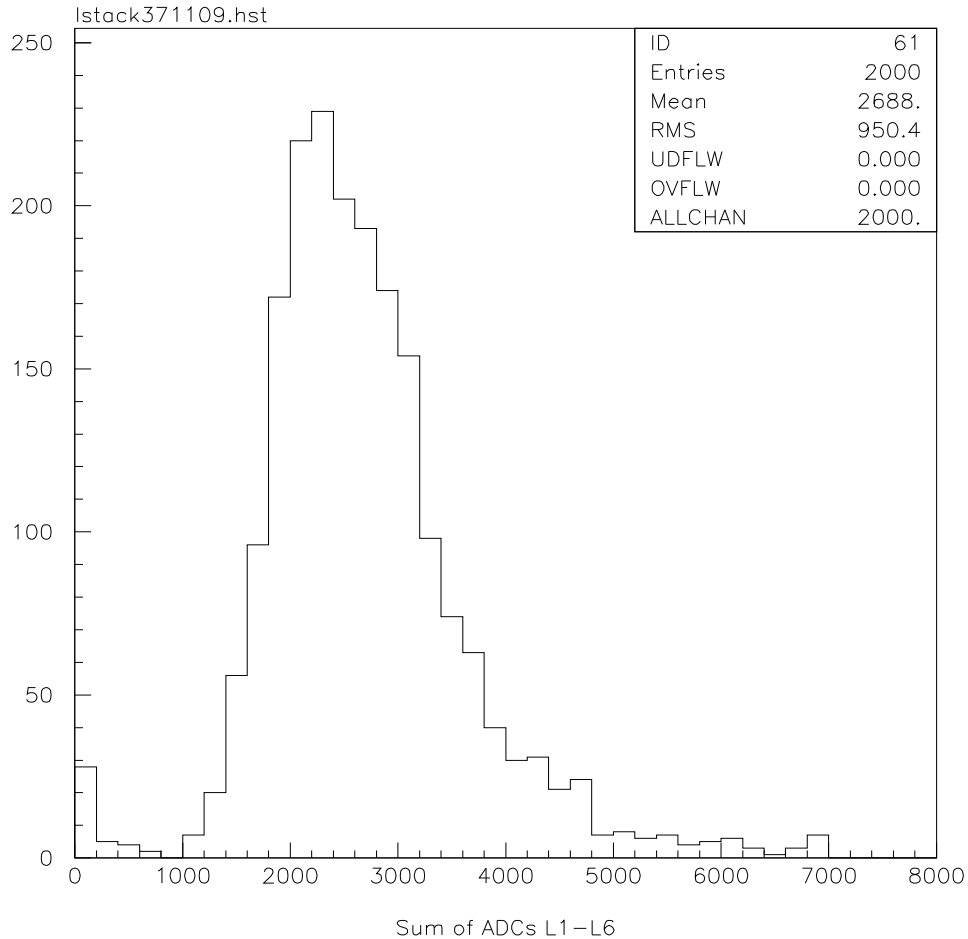


Figure 3: The sum of the ADC for the stack is displayed. This is from run 371109.

Figure 3 displays a typical spectra from such a requirement and shows a much sharper peak than the individual scintillators.

A run was performed with both LA and LB in the middle of the stack, and two runs with LB separated from the stack (60 and 150 cm). Some analysis was performed and discussed in the next section.

5 Data Processing and Manipulation

To examine the ADC and TDC information collected under various coincidence requirements a systematic procedure was developed. This procedure starts with the raw data and can produce histograms of data. Additionally various conditions may be specified in the software. For example, a “cut” on only specific events can be examined, or, as shown in Fig. 3, raw data may be added together. Curiously, some of the data showed events of an unknown origin, appearing as “zeroes” in the ADC and TDC.

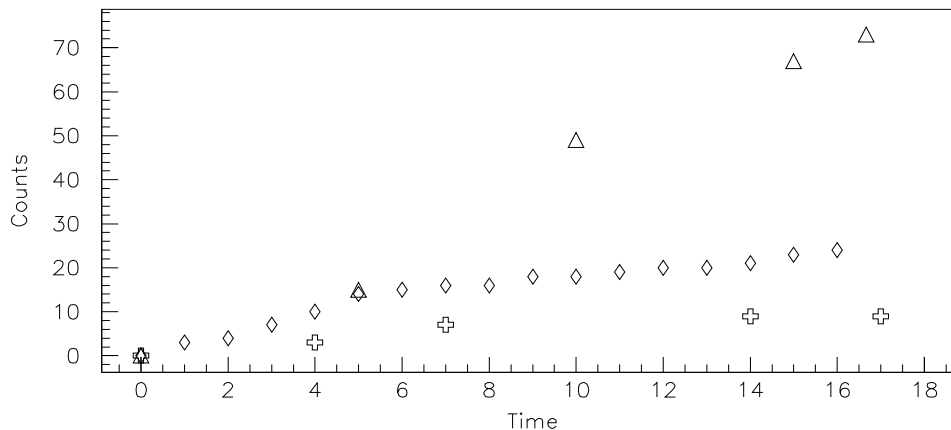


Figure 4: The three sets of data are for runs taken under identical conditions. The cause of the large variance is unresolved, but is suspected to be false zeros, and may be corrected for in software. See section 5.

This is an unresolved problem, however, these events may be removed by software cuts. It was noticed that they constitute a larger fraction of the events as coincidence detectors are placed farther apart. For instance, no events were discounted with LB on top of the stack, 40 out of 200 (20%) were discounted when LB was approximately 60 cm away from the stack center, and 117 (58.5%) when LB was 150 cm away. This suggested a study of the coincidence regularity. Three separate measurements were performed, and the number of coincidences (LA.LB.L1.L5) recorded against time. Each run was 1000 seconds. The data, which show vastly different count rates (under the same conditions!) are displayed in Fig. 4, and the data tabulated in table 2.

Again, these events and their origin is of interest, but for the present they may be discarded using software cuts.

6 LA.LB Measurements

A systematic study of the coincidence rates using LA and LB in various configurations was performed. In the first study the two detectors were placed side by side, such that the longer side of each was butted up against the other. Count rates were studied as a function of separation distance, where this distance is measured from the inside edge of one to the inside edge of the other. The data is presented in table 3. For most distances multiple measurements were made and a weighted average computed. The necessary formula is presented here. For further discussion of formula 3 refer to [6].

$$\begin{aligned}
 x_{ave} &= \frac{\sum \frac{1}{\sigma_i^2} x_i}{\frac{1}{\sigma_i^2}} \\
 \left(\frac{1}{\sigma_{ave}} \right)^2 &= \sum \frac{1}{\sigma_i^2}
 \end{aligned} \tag{3}$$

Three Counting Runs

Run One		Run Two		Run Three	
Time (min)	Counts	Time (min)	Counts	Time (min)	Counts
0	0	0	0	0	0
5	15	1	3	4	3
10	49	2	4	7	7
15	67	3	7	14	9
16.7	73	4	10	17	9
		5	14		
		6	15		
		7	16		
		8	16		
		9	18		
		10	18		
		11	19		
		12	20		
		13	20		
		14	21		
		15	23		
		16	24		

Table 2: Counts and cumulative time for three 1000-second runs. The trigger was LA.LB.L1.L6; LA and LB are approximately 150 cm apart.

LA.LB Separation Data

Separation (cm)	Coincidences/Minute	Error
0	52.0	2.79
10	25.4	1.95
50	7.42	0.86
100	5.48	0.30
145	2.18	0.21

Table 3: Displayed are coincidence rates as a function of the separation distance between scintillators LA and LB.

LA.LB Overlap Data		
Overlap (cm)	Coincidences/Minute	Error
35*	349.5	7.24
35	413.6	10.17
30	364.2	9.54
25	323.4	8.99
20	254.9	7.98
15	204.0	7.14
10	133.0	4.08
5	72.3	3.01
0	33.7	1.06
-10	14.5	0.70
-20	16.2	0.74

Table 4: Displayed are coincidence rates as a function of the overlap between scintillators LA and LB. All data taken with a 5 cm vertical separation except that listed in the first row (*), which was at 13 cm.

Error in counts is purely statistical (thus, $\sqrt{\text{counts}}$), error in time is negligible for Godwin and Langford, and no correlation is considered between the two detectors. The Raska data had some precise time measurements (*i.e.*, no error) and some measurements where the error in time was unknown. Times, precise to the minute, were given for the start and stop of these runs. An error of 90 seconds was assumed and added in quadrature to the count error. For long runs this is small, but for short runs (some only three minutes long) this became the dominant term. These data are plotted, along with previous measurements by Raska, in Fig. 5. There are a few data points from Lenka taken outside where the detectors are overlapping, and are included here.

Upon noticing that the coincidence rates are slightly larger in the present study, a series of overlap data were performed to see if the trend is the same. Table 4 presents these data. In this study it should be noted that the geometry is different. The overlap distance refers to the distance between the *ends* of the two scintillators whereas the previously presented data referred to the distance between the *sides* of the detectors. A negative value denotes a separation, but because of the geometry can not strictly be compared to the previously presented separation data (table 3).

Figure 6 graphically depicts this data. As can be seen, Godwin’s data is identical to Raska’s data, within error. However, an important consideration when performing these measurements is the *vertical* separation of the detectors. For that reason, Godwin took two “full overlap” measurements, one at 13 cm and one at 5 cm vertical separation. These data are also included in table 4 and demonstrates the solid angle consideration. Unfortunately, no information concerning the vertical separation is given by Raska, but it is conjectured that the two scintillators were directly on top of each other.

7 Models: Corsika and Others

One interest in studying cosmic rays is to understand the radial dependence of the shower, *i.e.* the location of the particles and gamma rays produced with respect to the path of the primary particle. Two papers were examined, one by Thompson [2], which is based on cosmic ray properties reported in the Particle Physics Booklet [7], and one by Wdowczyk [8]. The formula for the radial dependence in

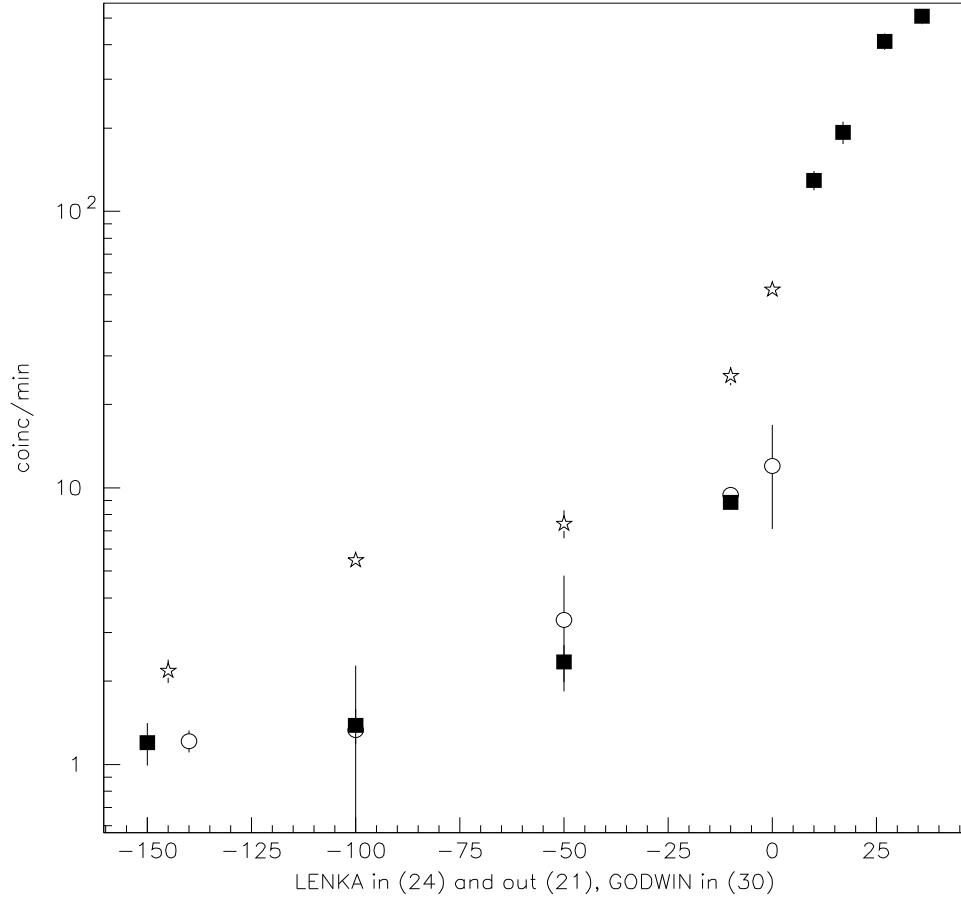


Figure 5: Separation data from Godwin, Langford and Raska. Godwin and Langford's data appear as stars and are all taken inside. Lenka's data are solid squares and open circles for her inside and outside measurements, respectively. Both set of data were taken with the LA (35cm x 17 cm) and LB (47cm x 17 cm) counters. Full cosmic ray flux through the area of LA (expected for the coincidence with no vertical separation) would be 10.7 particles/sec; for the "hard" (mostly muon) component only, the expected values would be 7.7 cts/sec. For a vertical separation of 4 cm the solid angle losses would be approximately 10%.

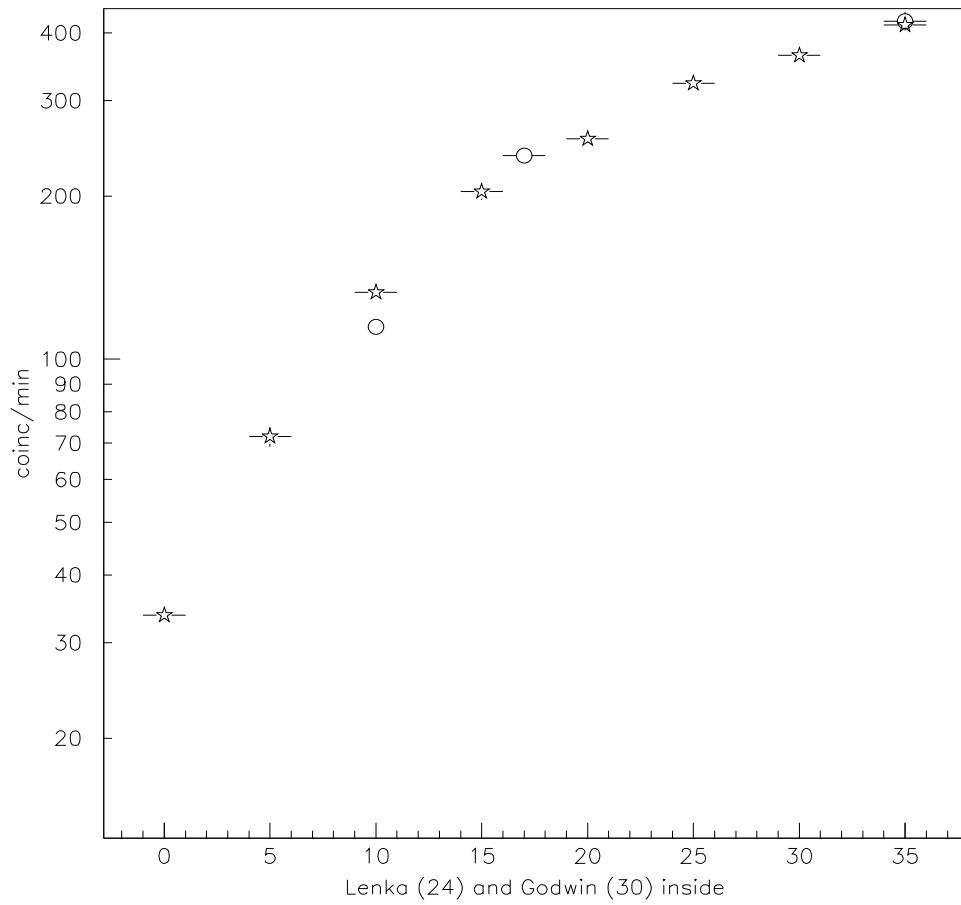


Figure 6: Overlap data from Godwin and Raska.

each case is presented in the paper, and for clarity is reproduced here. Thompson uses this equation:

$$\rho_{\mu} = \left(\frac{1.25 * N_{\mu}}{2\pi\Gamma(1.25)} \right) * (1/320)^{1.25} * r^{-0.75} * (1 + r/320)^{-2.5} \quad (4)$$

and Wdowczyk uses the following:

$$\rho_{\mu} = \frac{14.4r^{-0.75}}{(1 + r/320)^{2.5}} \left(\frac{N}{10^6} \right)^{0.75} \frac{51}{E + 50} \left(\frac{3}{E + 2} \right)^{0.14r^{0.37}} \quad (5)$$

The number of muons, N_{μ} , is arbitrarily assigned since only the radial dependence that is being considered here. In Wdowczyk's formula E is the energy of the muons at the ground. Sample data is shown below in Fig. 7 In this figure, the distribution of Thompson matches that of Wdowczyk at 1 GeV.

Julia Thomson has created numerous plots, from the simple model, to help understand how moun multiplicity, energy, and distance affect each other. These are presented:

Of course these are only simple accountings of a much more detailed physical process. The program Corsika [9] was used to obtain a more detailed understanding. This program, through a Monte-Carlo technique, allows the user to examine the outcomes of a cosmic ray and the shower it produces. The type, altitude, and energy of the primary may be adjusted at will. The program then estimates the production of gammas, muons, electrons, etc. at ground level. Figure 12 shows the number of photons, electron/positrons, muons, and hadrons at ground level, versus primary energy, assuming the shower is initiated in the upper atmosphere (a height of 113 km). The third plot shows a strong similarity between Corsika predictions (solid circles) and calculations based on the model described previously (open circles.)

Another interesting result from the Corsika shows the energy dependence of various shower products. In Fig. 13 five shower energies are chosen: 10^{15} , 10^{14} , 10^{13} , 10^{12} , and 10^{11} GeV. These are represented by the stars, crosses, diamonds, circles, and squares, respectively. For each one the number of particles produced (photons, electron/positons, muons, and hadrons) is graphed against the energy they possess at the ground. It is noticed that muons have a much greater energy than the electromagnetic component, and therefor suggests that shielding may help eliminate the soft component. The next figure (Fig. 14) shows a similar calculation, but this time plotting the number of particles against their distance from the central location, again for five shower energies. The significance of this is under investigation, along with further studies using Corsika.

8 Conclusions and Future Plans

Based on figures 13 and 14 a logical study would be to shield the scintillators from the electromagnetic flux. It is estimated that about 6 meters of iron would attenuate the electrons significantly while having little affect on the muons. Detectors could also be moved apart for further studies.

Plans are underway to place data in a publically viewable location. This data may be accessed and analyzed by students. For updates on this refer to the URL

<http://www.phyast.pitt.edu/~jth/CosRayHS.html>

Additionally, plans are underway for a larger project involving teachers and students for summer 2004. This website should be updated as plans are finalized.

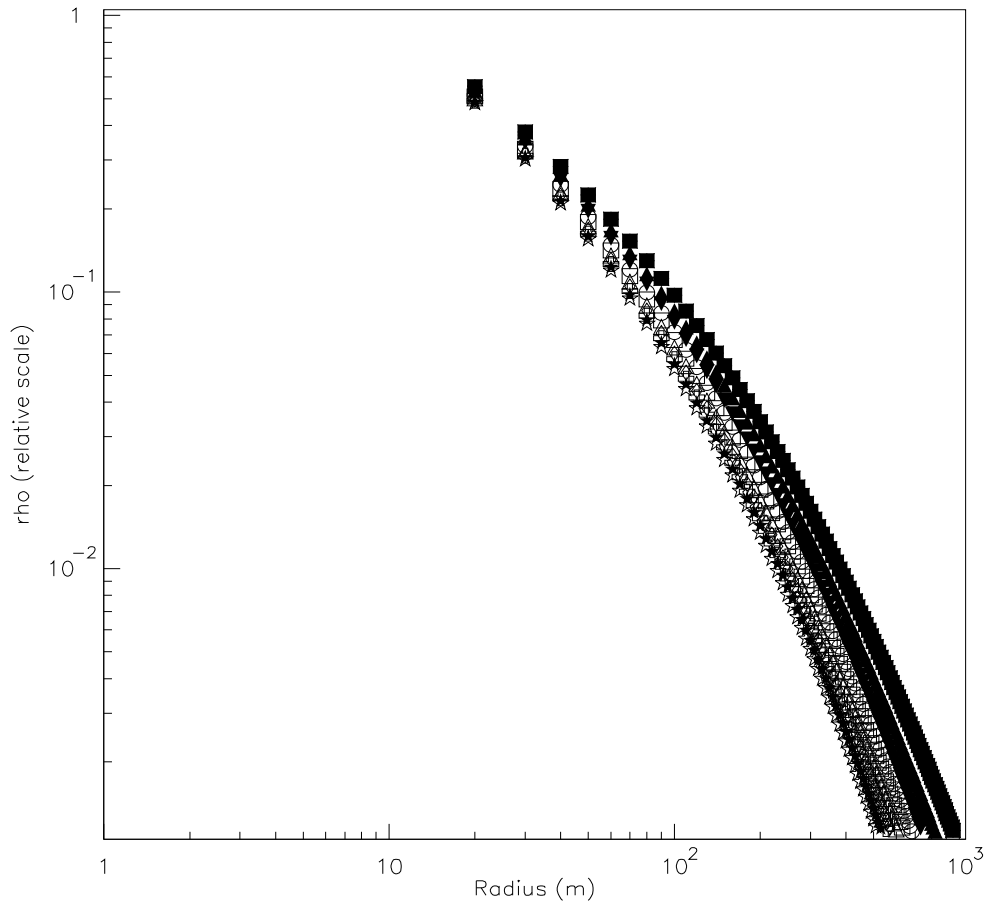


Figure 7: The figure shows the radial dependence of the muons from a shower. Muon energies of 1 to 10 GeV are displayed. All graphs are normalized to the same number at smallest radial measurement.

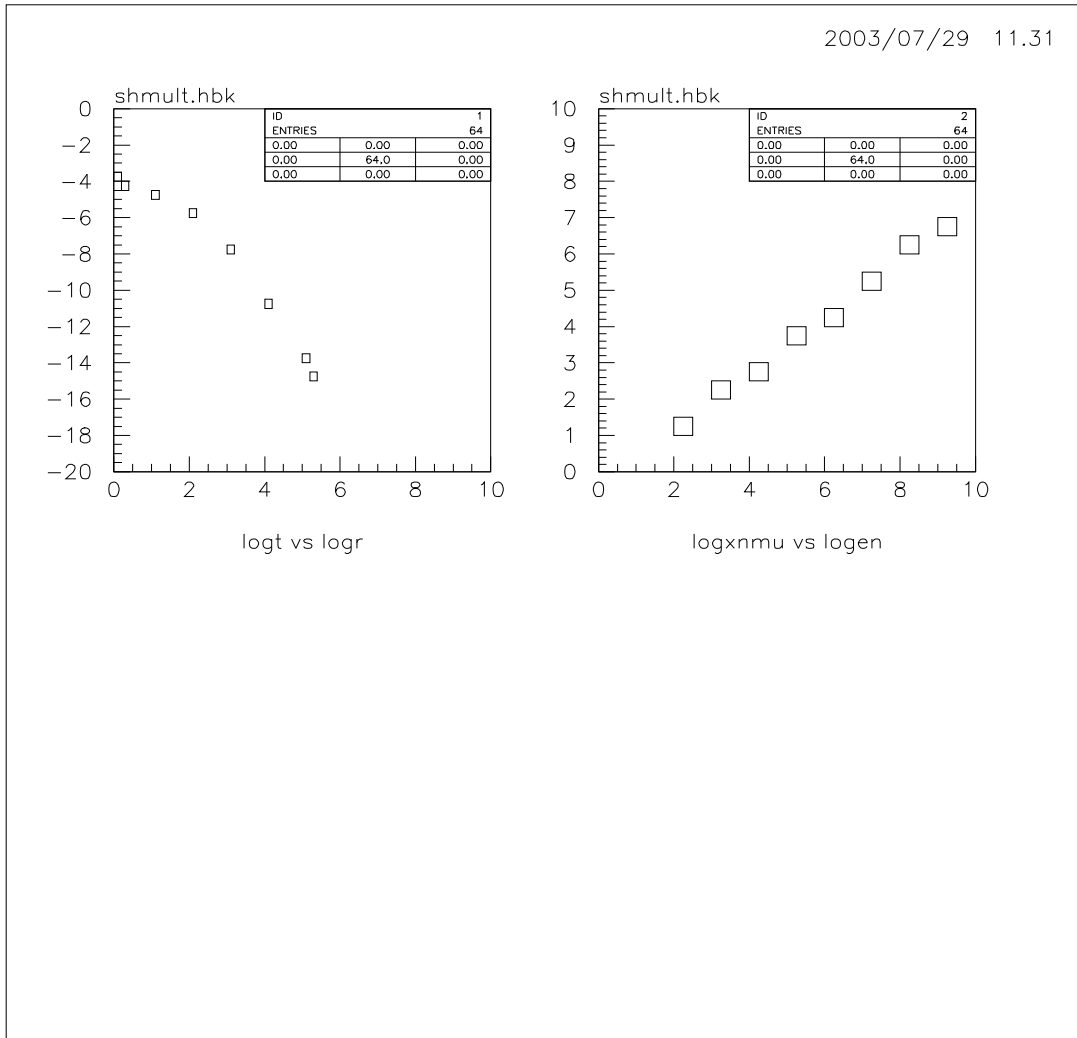


Figure 8: The first figure displays the radial dependence on the muon density, and the second the number of muons produced plotted against the cosmic-ray energy. The calculations use the “simple model” (see text).

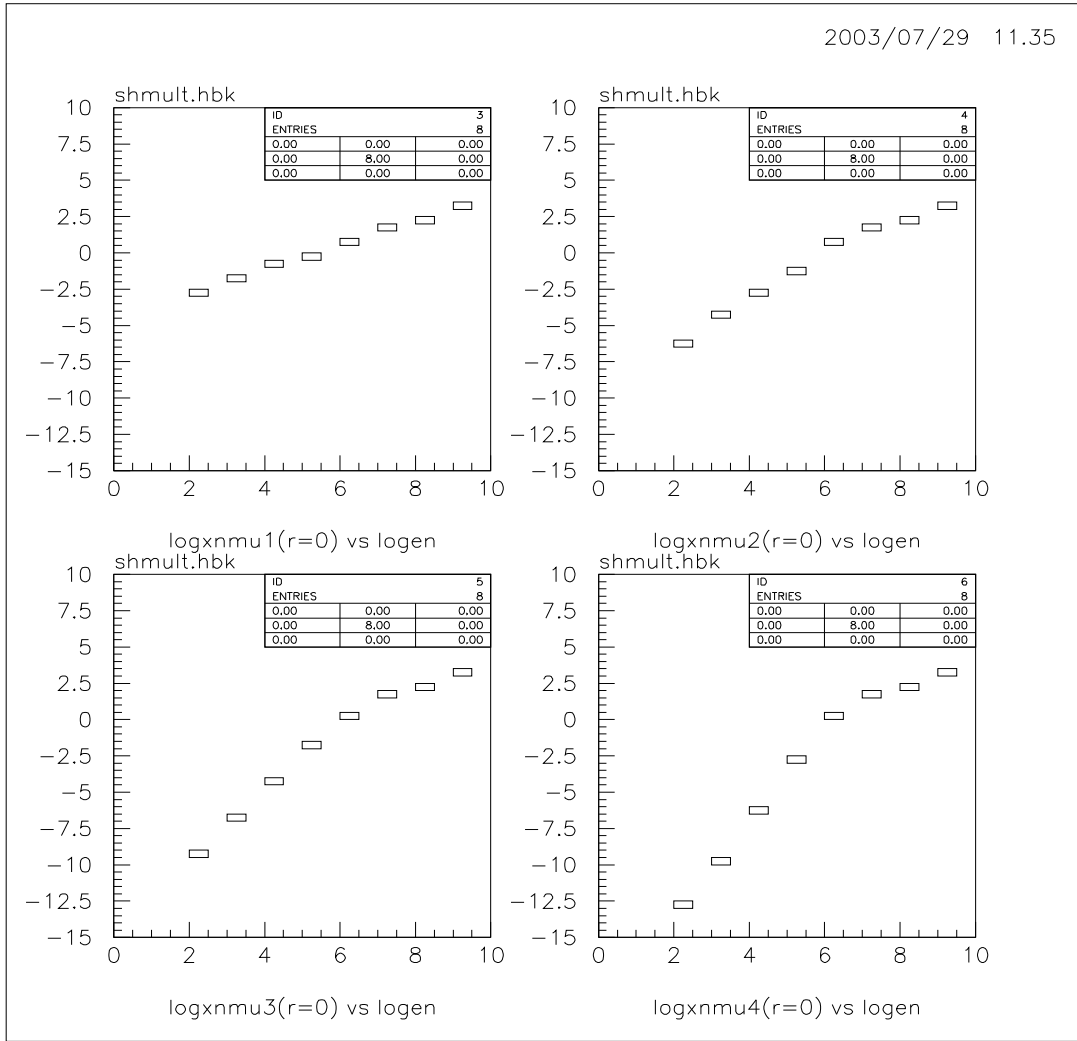


Figure 9: These plots show the muons density at $r=0$ against the shower energy, if a multiplicity of 1, 2, 3, or 4 is required. The calculations use the “simple model” (see text).

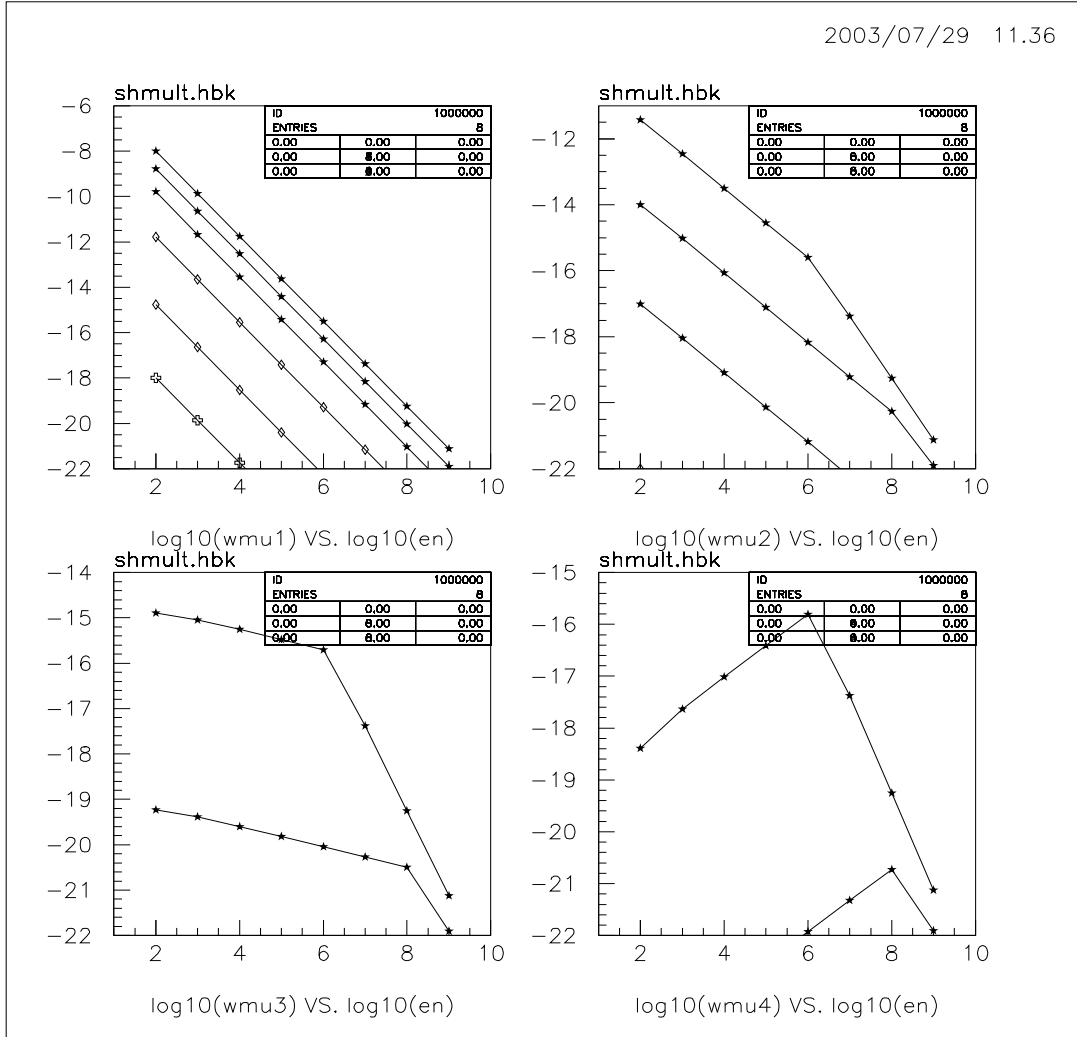


Figure 10: In each quadrant a family of curves is produced requiring different spacial separation of two $1m^2$ scintillators. Plotted on the ordinate is the multiplicity requirement and shower energy on the abscissa. The calculations are based on the “simple model” (see text).

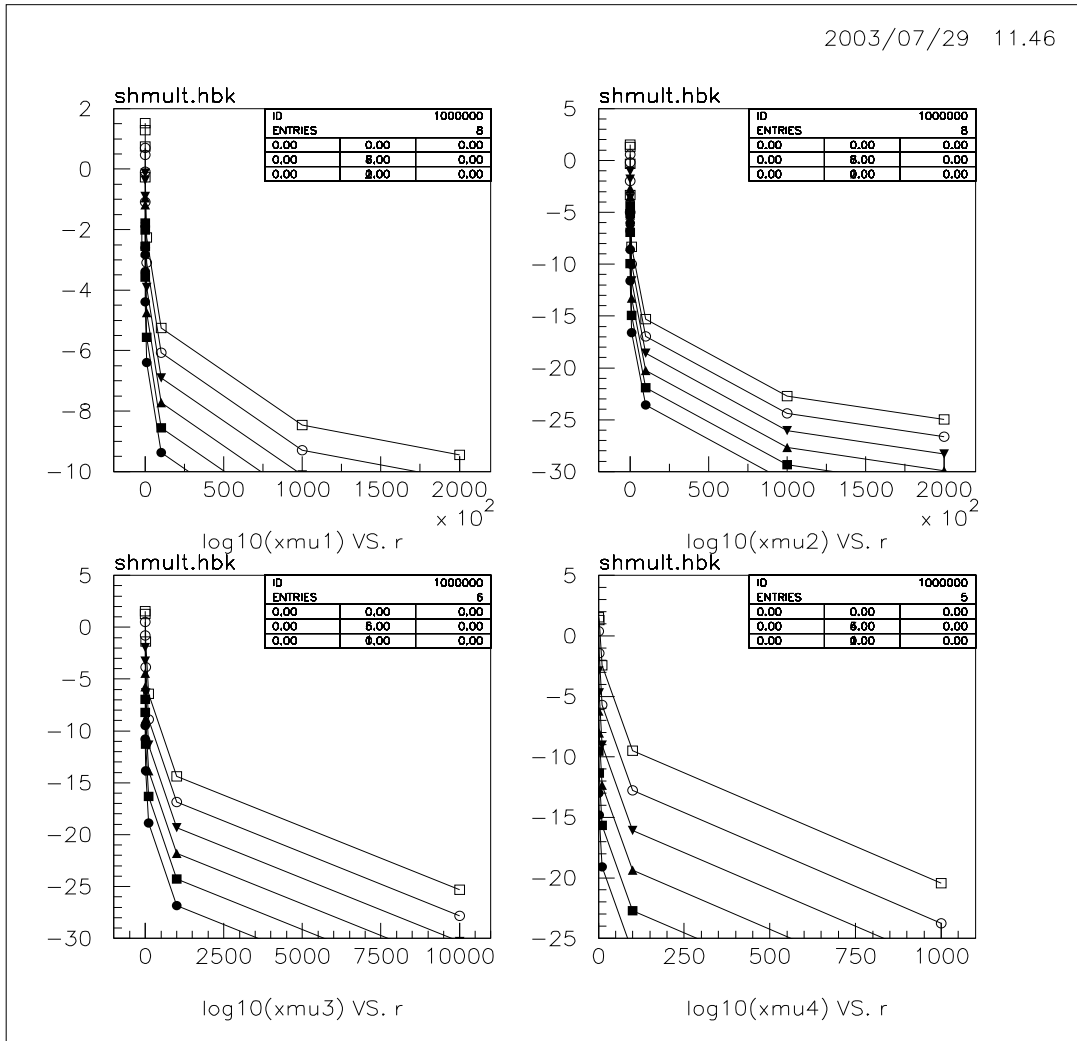


Figure 11: Using the “simple model” (see text), the muon density is plotted against radius for a multiplicity requirement of 1, 2, 3, or 4.

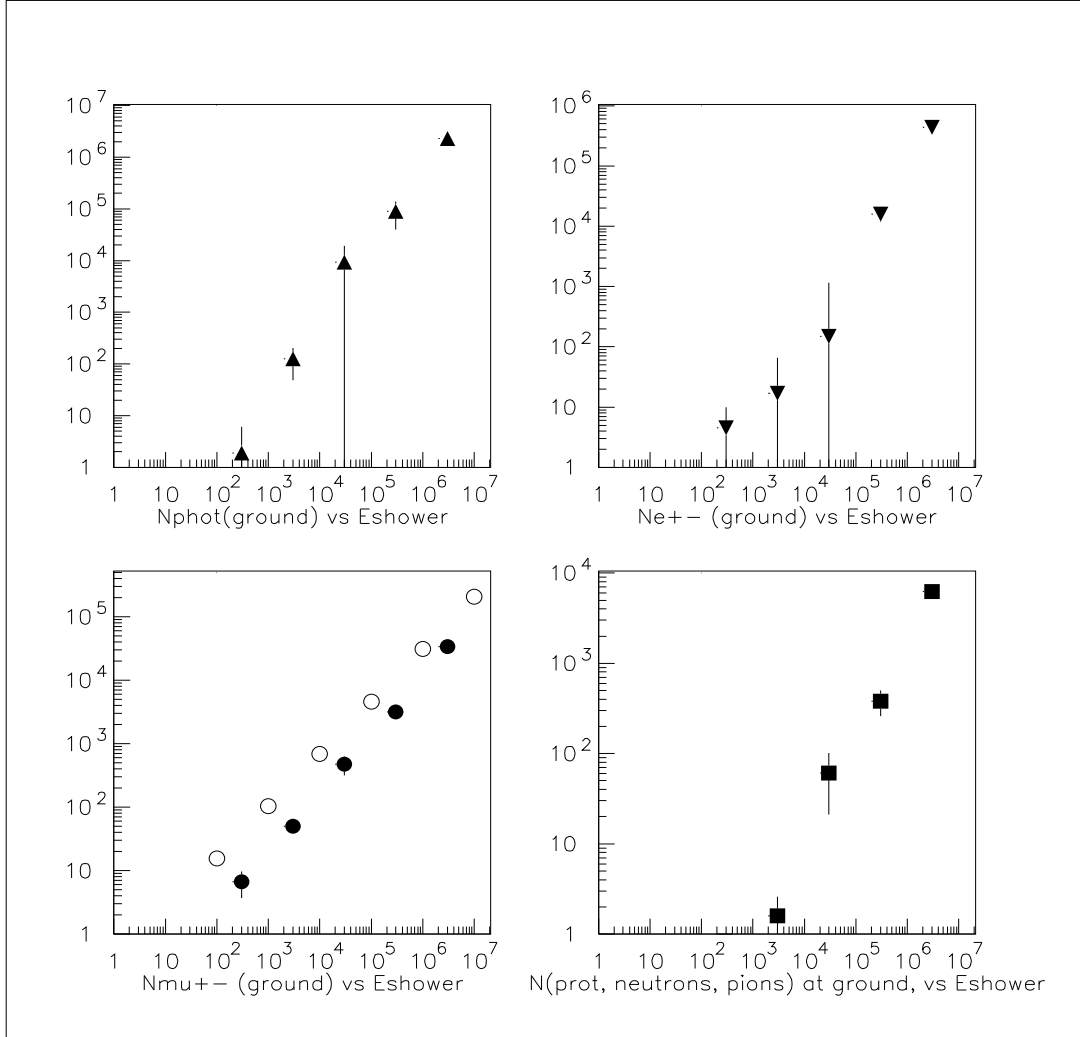


Figure 12: Shown are Corsika predictions for the multiplicity of photons, electron/positrons, muons, and hadrons at ground level, plotted against primary energy. The third graph also shows model predictions for muons as open circles.

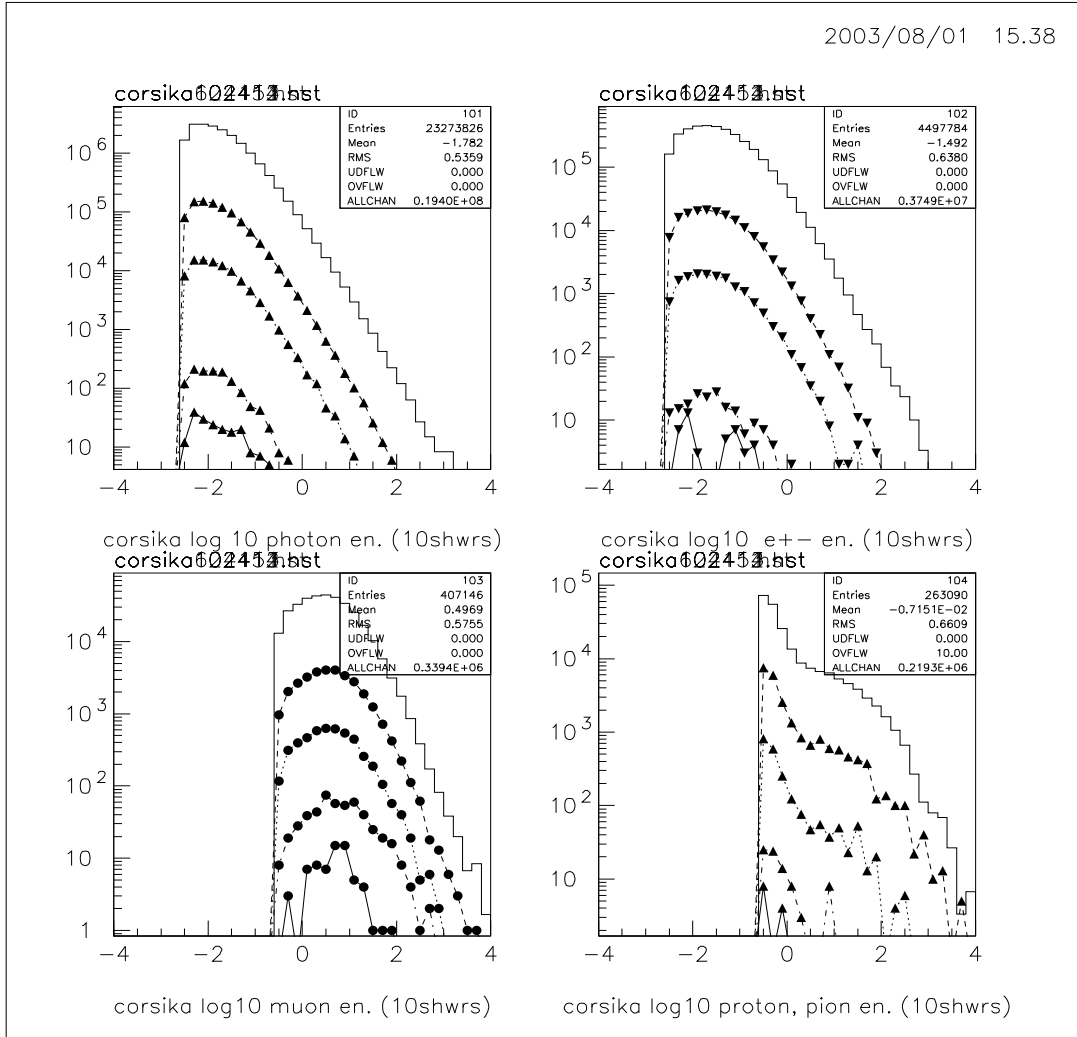


Figure 13: The plot shows the number of produced particles graphed against their energy for photons, electron/positrons, muons and hadrons. The stars, crosses diamonds, circles, and squares correspond to a primary energy of 10¹⁵, 10¹⁴, 10¹³, 10¹², and 10¹¹ GeV, respectively.

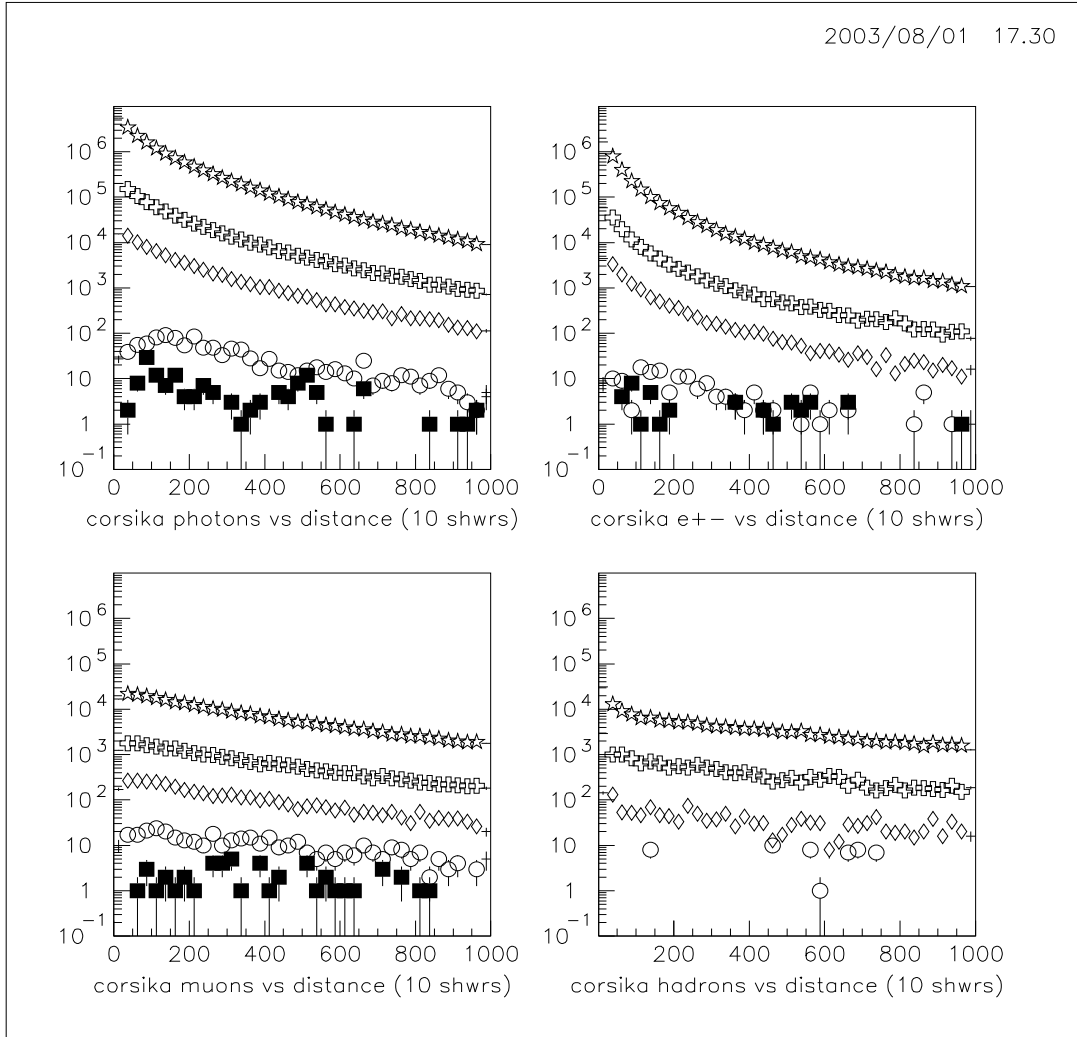


Figure 14: The plot shows the number of produced particles graphed against their radial distance for photons, electron/positrons, muons and hadrons. The stars, crosses diamonds, circles, and squares correspond to a primary energy of 10^{15} , 10^{14} , 10^{13} , 10^{12} , and 10^{11} GeV, respectively.

A 2003 Run Log

Below is the run log from 2003

Date	Run	Evts	Conditions, comments
July 2, 2003	3070201	100	LenkaA.L1.L6 prelim. volt. ~ 3.3/sec (ebl,jat)
	3070202	1000	LenkaB (for 1pe on LenkaB)
July 10, 2003	37102	1000	LA.L1.L6 (LA,LB ~ adjacent)
	37103	1000	LB.L1.L6 (LA,LB ~ adjacent)
	37104	1000	LA.L1.L6 (LA,LB ~ 1.5m sep)
July 11, 2003	37111	200	LA ~280/s (ebl,mg)
	37112	200	LB ~110/s
	37113	200	L1 ~600/s
	37114	200	L2 3.4k/s
	37115	200	L4 600/s
	37116	200	L5 10.5k/s
	37117	200	L6 1.4k/s
	37118	200	L5,tdc delayed 20ns 11.5k/s
	37119	2000	LA.L1.L6, LA near L1pmt 1.7/s
	3711A	2000	LB.L1.L6, LB near L2pmt 2.69/s
	3711B	2000	LB.L1.L6 LB,LA near center 3.65/s
	3711C	2000	LA.L1.L6 LB on table. 3.23/s
July 12, 2003			CHANGED RUN NUMBERS FROM JULY11. -MG
	37111 ==>	371101,	etc (so A,B,C, are 10,11,12)
July 14, 2003	37141	200	LA.LB.L1.L5, LA&LB in middle 0.19/s
July 15, 2003	37151	200?	LA.LB.L1.L5, LA-mid, LB-counter0.038/s LB next to stack (60cm)
	37152	200	LA.LB.L1.L5, LA-mid, LB-table 0.011/s LB on work table (150cm)
July 17, 2003	37171	???	LA.LB.L1.L5 0.57/min changed camlst so LAM is on ADC
	37172	???	LA.LB LA&LB in middle 58.14/min
July 23, 2003	xxxxx		Took a series of scalar readings for LA.LB
July 24, 2003	37241	400	LA.LB.L1.L5, LA&LB on sides 2.95/min
	37242	2000	LA.L1 535/min
	37243	2000	LB.L5 206/min
	37274	200	LA.LB.L1.L6 LA&LB on sides >2.14/min
July 26, 2003	37261	4000	LA.L1.L6 LA&LB on sides 4515/30min
	37262	4000	LB.L1.L6 LA&LB on sides 5207/30min
	37263	200	LA.LB.L1.L6 LA&LB on sides 74/30min

B Lenka Raska's Run Log

Presented are a non-exhaustive listing of Lenka's LA\@.LB data runs. The runs are categorized by separation or overlap distance as well as location (inside, outside). Further information may be found in the 2002 directory of kaon, and in Julia Thompson's notes.

Summary of Lenka's Separation Rates (2002)

Separation	RUN	CPM	Error	Notes
10 cm	58019	16	5	light on, maybe accidentals
	58020	8	2.828	lights off scalar data
	58020	9.545	0.2946	lights off, "1050 events in 110 minutes"
	58021	13	3.6	
	58034	6	3.46	outside
	58044	10.8	0.736	hall
	56005	2.55	0.075	with stack (trigger=A&B&[2 of 3 in stack])
	56010	8.93	0.35	
	56013	103	1.075	outside 3/6 large trigger
Weighted Ave & Error		9.436	0.214	
50 cm	58019(*)	3.33	1.49	
	58035	4	2.83	outside
	Weighted Ave & Error		3.33	1.49
100 cm	58036	1.33	0.943	outside
110 cm	58019(*)	3.6	1.2	
140 cm	56011	1.28	0.12	
	56006	9.2	0.083	with stack triggered on stack (see log)
	56007	0.87	0.275	(10 in "11-12 minutes")
150 cm	58037	1.2	0.2	outside
Weighted Ave & Error		1.21	0.1099	
300 cm	58006	0.833	0.0263	
400 cm	58022	0.55	0.034	
	58023	0.5633	0.0433	
0 cm	58014	12	4.9	

Summary of Lenka's Overlap Rates (2002 - Outside!)

Separation	RUN	Counts	Cnt Er	Time(s)	Tm Er	CPM	Error
36	58030	2000	44.72	180	90	666.7	333.667
36	58030	253	15.91	30	0	506.0	31.812
Weighted Ave & Error						507.5	31.668
17	58031	2000	44.72	420	90	285.7	61.557
17	58031	92	9.59	30	0	184.0	19.183
Weighted Ave & Error						193.0	18.315
27	58032	2000	44.72	300	90	400.0	120.333
27	58032	206	14.35	30	0	412.0	28.705
Weighted Ave & Error						411.4	27.922
10	58033	2000	44.72	900	90	133.3	13.663
10	58033	62	7.87	30	0	124.0	15.748
Weighted Ave & Error						129.3	10.320
-10	58034	535	23.13	3600	90	8.92	0.445
-10	58034	3	1.73	30	0	6.00	3.464
Weighted Ave & Error						8.87	0.442
-50	58035	51	7.14	1320	90	2.32	0.361
-50	58035	2	1.41	30	0	4.00	2.828
Weighted Ave & Error						2.35	0.358
-100	58036	50	7.07	2160	90	1.39	0.205
-100	58036	2	1.41	90	0	1.33	0.943
Weighted Ave & Error						1.386	0.200
-150	58037	36	6.00	1800	90	1.20	0.209

C Data Processing Procedure

(Created on: 15 July 2003)

(Revised on: 16 July 2003)

(Created by: Mark Godwin)

(Notes: Taken from coswork/2003/log/2003log.txt file)

*** First copy data from CAMAC computer to Kaon:

1. Copy to a disk from dtake computer (in dos, copy filename a:)
2. Change directory to desired (e.g. cd coswork/2003/stack+2/)
3. Enter superuser mode by doing (type: su) then enter password
4. Copy files from disk to kaon (e.g. mcopy a:RUNXXXXX.DAT RUNXXXXX.DAT)
5. Change ownership (e.g. chown cosray:cosray RUN*.DAT)
6. Exit superuser mode (type: exit)

*** Next "process" the data:

1. pico ereadnjt.c (and change run number on line 10)
2. clgcern lstack ereadnjt.c > lstackXXXXXX.log (compiles, puts output into lstackXXXXXX.log file)
3. mv lstack.hst lstackXXXXXX.hst (renames histogram file)
4. pico lstack.paw (and change run number on line 1)
5. pawlstack.com XXXXXX > pawlstack.log (creates postscript file)

Note: This can give an error message, but that's OK

/bin/mv: cannot stat 'lstackXXXXXX.ps': No such file or directory

6. gv lstackXXXXXX.ps (look at output using ghostview)
7. ps2pdf lstackXXXXXX.ps lstackXXXXXX.pdf (creates pdf file for easy printing)

D Plotting with PAW

This procedure will read in ntuples from previously made .hst files and plot multiple runs on one page or even multiple histograms on the same plot. References to making the histogram files in the first place may be found in appendix~\ref{app:dataprocessing}

Create a new kumac file called "special.kumac", edit it, change gen.paw (a GENERAL paw file), and the paw gen.paw. Following are sample steps where the new process is called "special"

1. cp whatever.kumac special.kumac (creates a new .kumac from an existing one ==> CAREFUL, DON'T ****mv**** file)
2. pico special.kumac (edit new .kumac file)
 - a. Make changes as desired
You should rename the macro to "special", as shown below
 - b. macro special (line 1)
 - c. fort/file 2 special.ps (line 8, but this might vary)
3. pico gen.paw (change name on first line to special)
4. pawgen.com gen.paw > gen.log (pawgen.com "paws" gen.com)(or call log file special.log)
5. view postscript (the name for the postscript is in the .kumac file. See step 2c)
 - 5b. If in computer lab, you need to telnet to Kaon, ftp to jinx, put file into jinx, then use ftp from start menu, log on to jinx, transfer file to harddrive, and view. At present I installed ghostview onto computer BH23212

To make plots of data generated elsewhere (such as Excel, etc) use the same procedure, but you'll need to add the data to the kumac. One typical command would be:

```
ve/cre run1datatime(5) R 0 5 10 15 16.67
```

This creates a vector, 5 real entries.

E Move and Print Files

This logs in to your account, and then logs into Kaon: (Mark's way)
To move files FROM Kaon to jinx do the following:

1. Select telnet from the start menu
(start/programs/The Internet/telnet)
host: jinx
user: magrg7 (or your account name)
select Connect, then select No
password: <<yourpassword>>
2. At jinx% prompt type this:
jinx% ssh -l cosray r403hp3.umsl.edu
password: <<the password for the "cosray" account on the computer
"r403hp3.umsl.edu" - (see Julia or Kari)>>
3. Change directory to where ever you want, for example
cd coswork/2003/stack+2/
4. Now to transfer files, use ftp
ftp jinx.umsl.edu
name: magrg7 (or your account name)
password: <<yourpassword>>
ftp> change directory (e.g. cd mycosray)
ftp> put <<filename>> <<newfilename>> (defaults to same)
ftp> quit (exit to get back into your jinx account)
5. The file is in your jinx account. Now print it!
lpr -Ptxbh232 <<filename>> (**for a text file**)
lpr -Ppsbh232 <<filename>> (**for a postscript file**)

References

- [1] Elisabeth Langford, "LANGFORD'S TITLE", Report for R.E.T program, UMSL, July 2003.
- [2] Oluwafemi Osidipe, Drew Thomas, Elizabeth Weber, Julia Thompson and Dave Kraus, "Cosmic Ray Project", Report for R.E.T program, REUP-FOM/SIUE, June 11 2001.
- [3] Lenka Raska, "Cosmic Ray Telescope", Report for R.E.T program, USIE, August 2002.
- [4] Steve Grosland, "Cosmic Ray Studies", Report for R.E.T program, UMSL, July 2003.
- [5] Dave Kraus, Personal Communication.
- [6] Philip R. Bevington, D. Keith Robinson, Philip Bevington, **Data Reduction and Error Analysis for the Physical Sciences**, McGraw-Hill Science/Engineering/Math (2002).
- [7] Particle Data Group, "Particle Physics Booklet", American Institute of Physics, July, 1996.
- [8] J. Wdowczyk, **Extensive air showers below 10^{17} eV**, PUBLISHER (1973).
- [9] Corsika Users Manual or something like that .